Peremennye Zvezdy (*Variable Stars*) **44**, No. 2, 2024

Received 15 March; accepted 12 April.

DOI: 10.24412/2221-0474-2024-44-6-27

Seven New Multiperiodic δ Scuti stars in Cygnus

A. Samokhvalov

Surgut, Russia, e-mail: sav@surgut.ru

In a small field in Cygnus, I discovered seven new DSCTC stars that demonstrate multiperiodic pulsations from V-band CCD observations. For each of these stars, from two to four reliable pulsation frequencies could be derived. The paper presents finding charts, frequency spectra, light curves for program stars. New high-quality multi-band observations of the discovered variable stars with larger telescopes are needed.

1 Introduction

Working on our program aimed at discoveries and studies of DSCT-type stars, we have discovered seven new DSCTC stars with signs of multiperiodic pulsations in a field in Cygnus. The main information about these stars is presented in Table 1. Their coordinates were drawn from the Gaia DR3 catalog (Gaia Collaboration, 2022). None of these stars are currently contained in the General Catalogue of Variable Stars (GCVS), see Samus et al. (2017), or in the AAVSO Variable Star Index (VSX), see Watson et al. (2006). However, they are marked VARIABLE in the Gaia DR3 catalog, see Gaia Data Release 3 (Gaia DR3), Variability (Eier et al., 2023). Infrared color indexes were drawn from 2MASS catalogue (Cutri et al., 2003).

Table 1. New Variable Stars

No.	USNO-A2.0	RA, J2000.0	Dec, J2000.0	V	$J-H$	$H-K$	$J-K$
1	1425-12331125	$21^h47^m03^s.921$	$+53°45'36''.89$	$15^m.40-15^m.48$	$0^m.431$	$0^m.152$	$0^m.583$
2	1425-12332333	21 47 07.191	+53 53 01.42	12.33 – 12.38	0.269	0.083	0.352
3	1425-12344159	21 47 39.389	+53 57 04.09	12.53 – 12.65	0.388	0.205	0.593
4	1425-12354548	21 48 08.497	+53 34 46.28	13.50 – 13.54	0.196	0.111	0.307
5	1425-12372223	21 48 58.784	+53 57 17.33	15.73 – 15.90	0.377	0.165	0.542
6	1425-12374410	21 49 05.085	+53 53 57.54	14.31 – 14.38	0.374	0.165	0.539
7	1425-12377701	21 49 14.504	+53 30 36.92	15.16 – 15.24	0.428	0.130	0.558

Based on VSX and 2MASS catalogs, we plot a population distribution diagram of DSCT stars (DSCT, DSCTC, and HADS-type stars) as a function of infrared colors, derived from 2MASS photometry (Fig. 1). Only stars with good 2MASS photometry ($Qflg = AAA$) and reliably defined variability types (without an uncertainty symbol ":" in VSX Type) are used. All the new variable stars reported here also possess the 2MASS quality flag $Qflg = AAA$. The new variable stars are located in this diagram near the maximum-density population core, in the green and blue zones. This position can be considered one of the signs of belonging to the DSCT variability type.

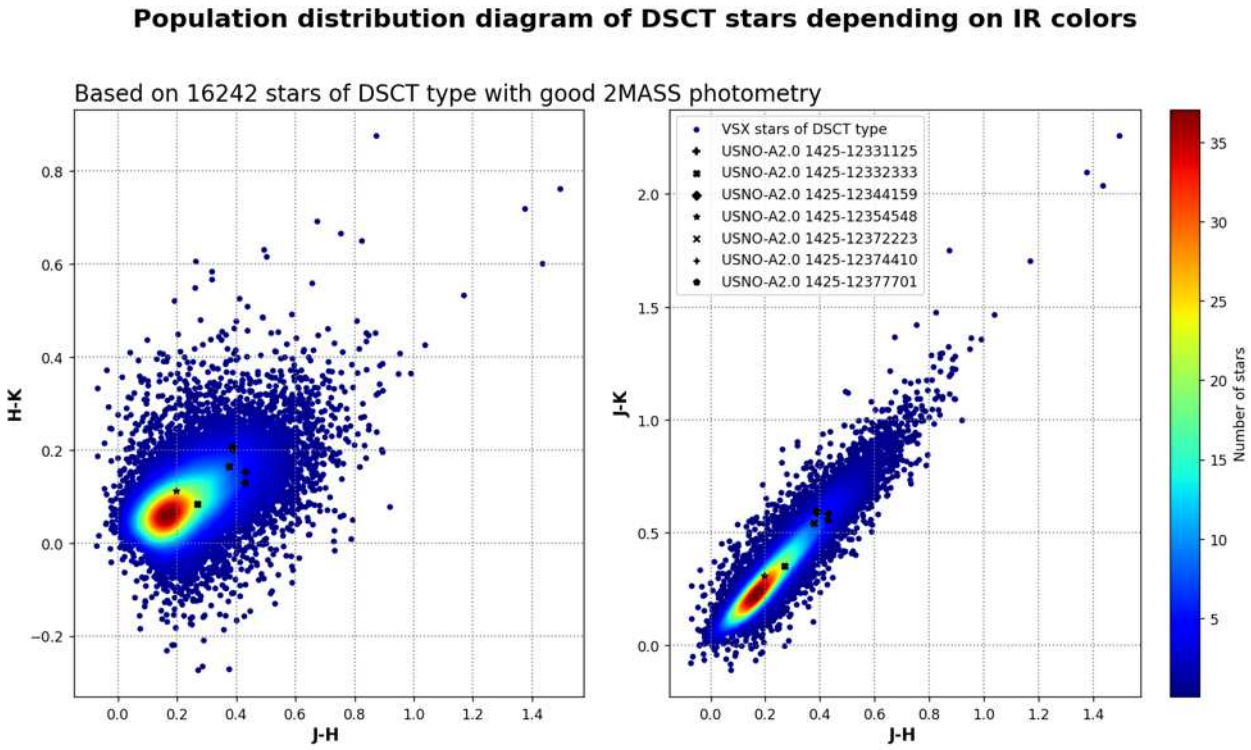

Figure 1.
Population distribution diagram of DSCT stars as a function of 2MASS infrared colors $H-K(J-H)$ and $J-K(J-H)$. New variable stars are marked in the diagram.

2 Observations, primary reduction and magnitude calibration

Our observations were carried out at the Caucasian Mountain Observatory (CMO) of M.V. Lomonosov Moscow State University (Shatsky et al., 2020) using the 0.25-m remote-controlled Ritchey–Chretien telescope, equipped with a SBIG STXL-6303e CCD Camera and a V filter. A total of 1120 images of the field with 600-second exposures were obtained on JD 2460187–2460325. Information about the number of images taken on each observing night is given in Table 2.

Table 2. Images taken on each observing night

HJD	Images	HJD	Images	HJD	Images	HJD	Images	HJD	Images
2460187	12	2460211	27	2460237	33	2460259	33	2460302	4
2460188	9	2460212	4	2460238	30	2460261	13	2460308	23
2460189	15	2460216	25	2460240	29	2460275	5	2460309	6
2460190	14	2460218	32	2460246	21	2460277	31	2460310	9
2460198	22	2460223	9	2460248	35	2460281	37	2460311	21
2460202	18	2460225	33	2460249	32	2460282	15	2460314	14
2460203	16	2460226	6	2460250	19	2460283	36	2460316	18
2460207	23	2460230	30	2460253	31	2460286	5	2460320	22
2460208	25	2460231	30	2460254	15	2460287	5	2460321	21
2460209	26	2460232	30	2460256	12	2460298	28	2460325	17
2460210	28	2460233	30	2460257	11	2460299	25		

For basic reductions for dark current, flat fields, and bias, and in order to remove hot pixels and cosmic rays hits, we used IRAF routines and proprietary software TheSkyX™by Software Bisque Inc. For calibration, each observing night we obtained 16 bias frames,

16 dark frames, 16 flat fields, plus 16 dark frames corresponding to flat fields.

For photometry of new pulsating stars, we applied VaST software by Sokolovsky and Lebedev (2018). All times in this paper are expressed in terrestrial time in accordance with IAU recommendations (resolution B1 XXIII IAU GA), with heliocentric corrections applied.

For magnitude calibration in the V band, we use data of the GAIA DR3 catalogue. We restrict ourselves to single, relatively bright stars, with no saturation of pixels for our CCD camera, no close neighbors, and demonstrating no brightness variations during the time interval of our observations. Detailed information about our calibration stars is collected in Table 3. Uncertainties in the σ_V column were derived from our photometry, the GAIA G, G_{BP}, and G_{RP} magnitudes were drawn from the corresponding catalog. Magnitudes in the "Calc. V" column were obtained using the equation:

$$\text{Calc. } V = \text{Gaia } G - [-0.02704 + 0.01424 \times (G_{BP} - G_{RP}) - 0.2156 \times (G_{BP} - G_{RP})^2 + 0.01426 \times (G_{BP} - G_{RP})^3], \quad (1)$$

which is based on table 5.9 of the Gaia Data Release 3, Documentation release 1.2 (https://gea.esac.esa.int/archive/documentation/GDR3/)

Table 3. Magnitudes of calibration stars

GSC	σ_V	GAIA			Calc. V
		G	G_{BP}	G_{RP}	
3968-2621	0.008	11.5102	12.5060	10.5323	12.2394
3968-3272	0.007	12.1790	12.5445	11.6340	12.3610
3968-3000	0.008	12.3394	12.5281	12.0156	12.4139
3968-2894	0.007	12.0446	12.3314	11.5923	12.1732
3968-2595	0.007	11.8378	12.1974	11.3031	12.0143
3968-2517	0.007	12.0227	12.2059	11.7003	12.0958

The observations are presented as a zip archive in the html version of this paper.

3 Results

To derive periods, we use Period04 software by Lenz and Breger (2005) that implements the discrete Fourier transform, very suitable for analysis of sine-shaped light curves of the pulsating variable stars with multiperiodicity.

We searched for periodic signals in our observations in the frequency range between 3 and 20 cycles per day that was selected following recommendations by Breger (2000). We continuously calculate significant frequencies, in the first iteration based on the original data, in the following iterations, using residuals instead, as long as the signal-to-noise ratio for the corresponding peak in the Fourier frequency spectrum exceeds 4. This is the empirical criterium obtained from the analysis of observations by Breger et al. (1993) and ensuring that the signal is a real feature. Parameters of the oscillations corresponding to the equation

$$m(t) = m_{mean} + \sum A_i \sin(2\pi(f_i t + \Phi_i)) \quad (2)$$

were determined by least squares and are collected in Table 4. The first column of this table gives the star's number in the USNO-A2.0 catalogue (Monet et al., 1998). The second column is the number of photometric measurements for the corresponding star. The third column is the average error of photometrical measurements. The fourth column contains the mean magnitude corresponding to Equation 2. Subsequent columns describe oscillations of each star. The column named $Freq_i$ contains numbers of significant

frequencies, which are presented in the next column. Columns marked Φ_i and A_i contain the phase and amplitude of the ith oscillation. In the last column, we give the S/N ratio for the ith frequency, derived using the Period04 software. Only frequencies that satisfy the $S/N > 4$ criterion are kept.

For plotting light curves, Fourier spectra, and population distribution diagram, we used our own routines written in Python 3 programming language using the NumPy (Harris et al., 2020) and Matplotlib (Hunter, 2007) libraries.

Table 4. Detected frequencies of the new pulsating variable stars

USNO-A2.0	N	m_{error}	m_{mean}	Oscillations				
				$Freq_i$	Frequency, d^{-1}	Φ_i	A_i, mag	SNR
1425-12331125	986	0.012	15.4382	f_1	7.17082	0.11158	0.0213	23.48
				f_2	8.46182	0.33195	0.0042	4.80
1425-12332333	1051	0.0018	12.3762	f_1	5.841265	0.28593	0.0123	26.98
				f_2	5.503670	0.91417	0.0060	12.73
				f_3	7.543690	0.55110	0.0039	10.27
				f_4	6.930815	0.05636	0.0031	7.91
1425-12344159	1054	0.013	15.5964	f_1	11.349167	0.16114	0.0173	15.00
				f_2	6.429910	0.95664	0.0163	12.13
				f_3	11.116893	0.30195	0.0104	8.99
				f_4	11.034570	0.09757	0.0066	5.63
1425-12354548	1057	0.0033	13.5234	f_1	17.932155	0.85287	0.0107	30.26
				f_2	18.073310	0.02408	0.0037	10.46
				f_3	13.329770	0.57958	0.0019	5.45
				f_4	14.873727	0.49255	0.0018	5.13
1425-12372223	1059	0.0156	15.8190	f_1	8.979444	0.15165	0.0285	23.99
				f_2	8.713564	0.07668	0.0270	22.54
				f_3	9.410159	0.43088	0.0196	16.52
				f_4	17.201639	0.96931	0.0085	7.70
1425-12374410	1058	0.0054	14.3492	f_1	12.666880	0.58088	0.0159	21.03
				f_2	12.963420	0.33383	0.0084	10.76
1425-12377701	1054	0.0097	15.2028	f_1	17.573930	0.13065	0.0159	24.92
				f_2	14.945790	0.93866	0.0080	10.64
				f_3	14.717230	0.02628	0.0045	5.92

Our observations are available as a zip archive in the html version of this paper.

3.1 USNO-A2.0 1425-12331125

This is the faintest star in our sample, and we found only two significant frequencies for it. The second frequency has a very small amplitude and is very close to the lower reliability boundary, with the S/N ratio 4.8.

Figure 2 presents the frequency spectrum of USNO-A2.0 1425-12331125 and its theoretical light curve (solid curve) with superposed data points corresponding to individual observations.

The finding chart based on a POSS2 red plate is presented in Fig. 3.

The V-band phased light curve of USNO-A2.0 1425-12331125 with the following light elements:

$$\text{Max HJD(TT)} = 2460231.4118 + 0\overset{\text{d}}{.}139454 \times E$$

is presented in Fig. 4.

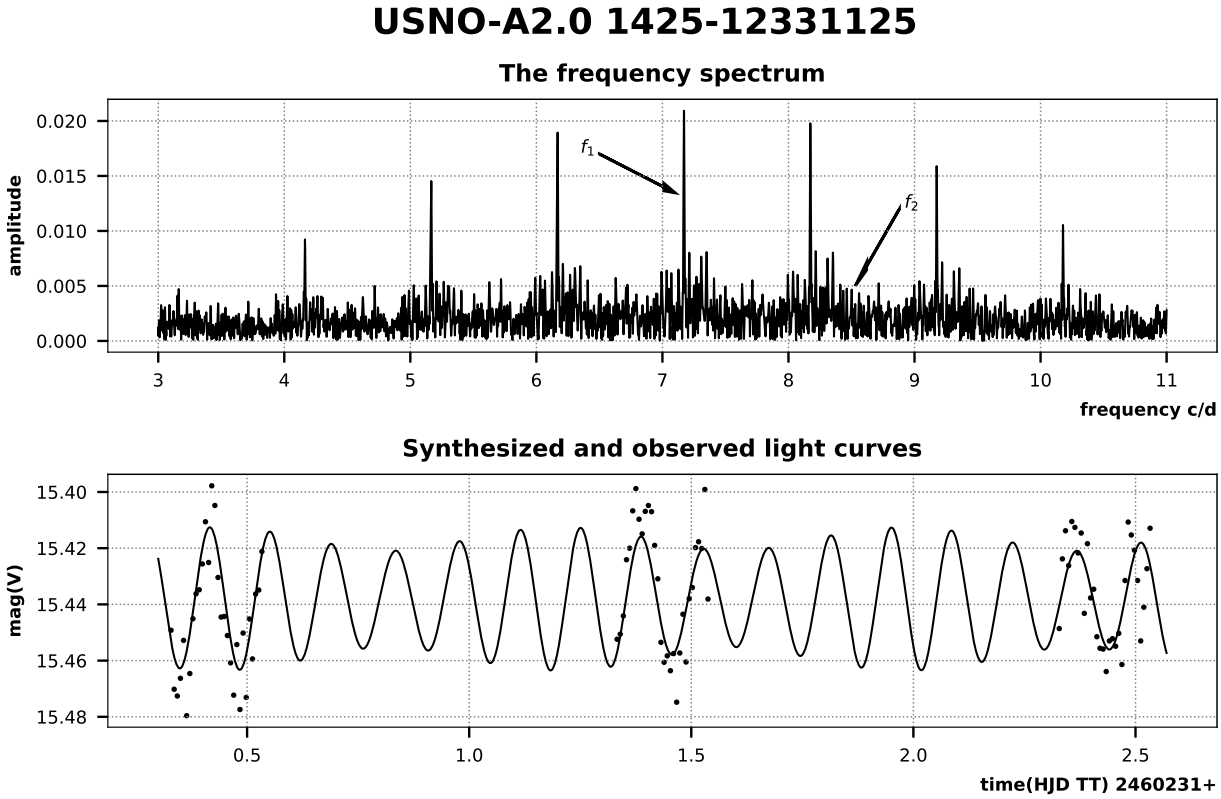

Figure 2.
The frequency spectrum and light curve of USNO-A2.0 1425-12331125. In the bottom panel, the solid curve is the synthesized light curve and dots are observed data points.

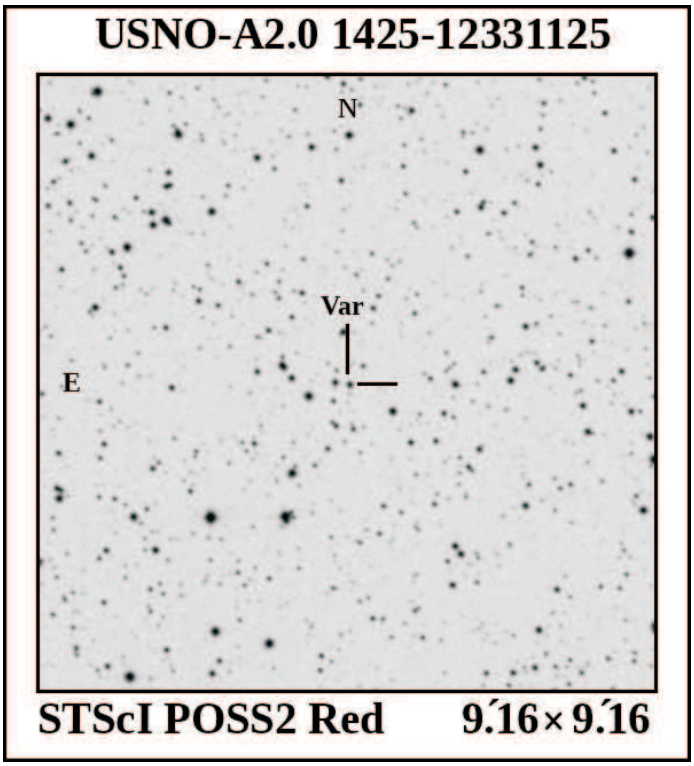

Figure 3.
A finding chart for USNO-A2.0 1425-12331125.

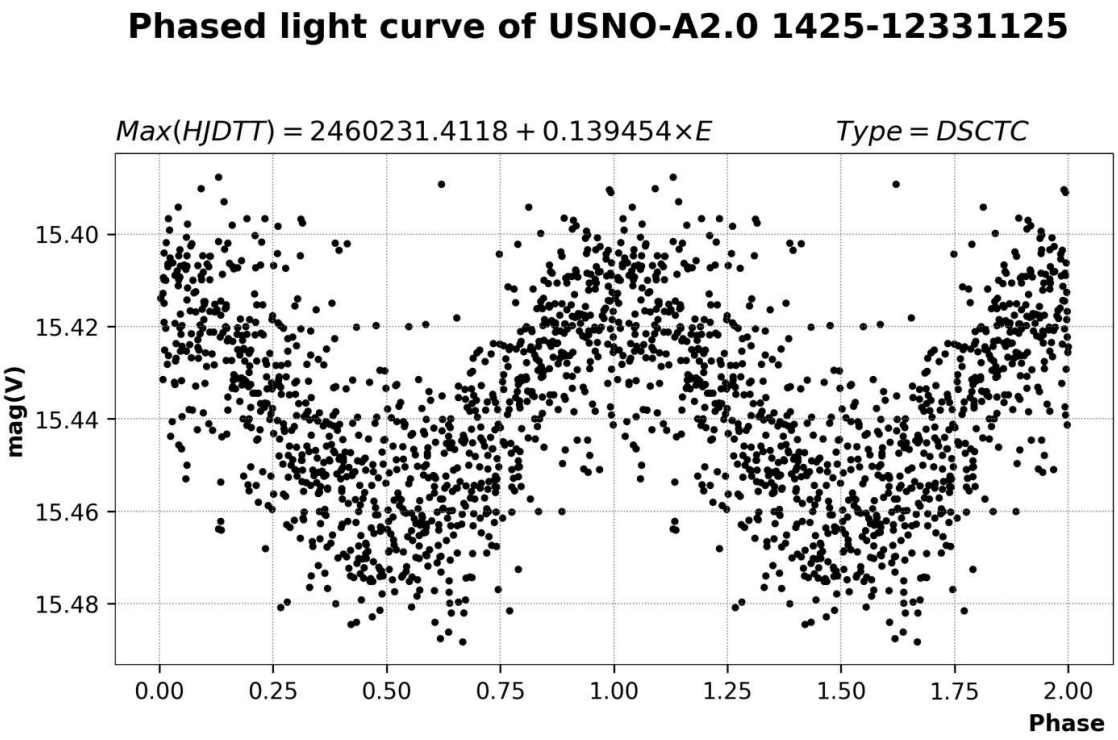

Figure 4.
Phased light curve of USNO-A2.0 1425-12331125.

3.2 USNO-A2.0 1425-12332333

Figure 5 presents the frequency spectrum of USNO-A2.0 1425-12332333 and its theoretical light curve (solid curve) with superposed data points corresponding to individual observations. Light curve variations are easy to notice, they are reproduced with the model rather well.

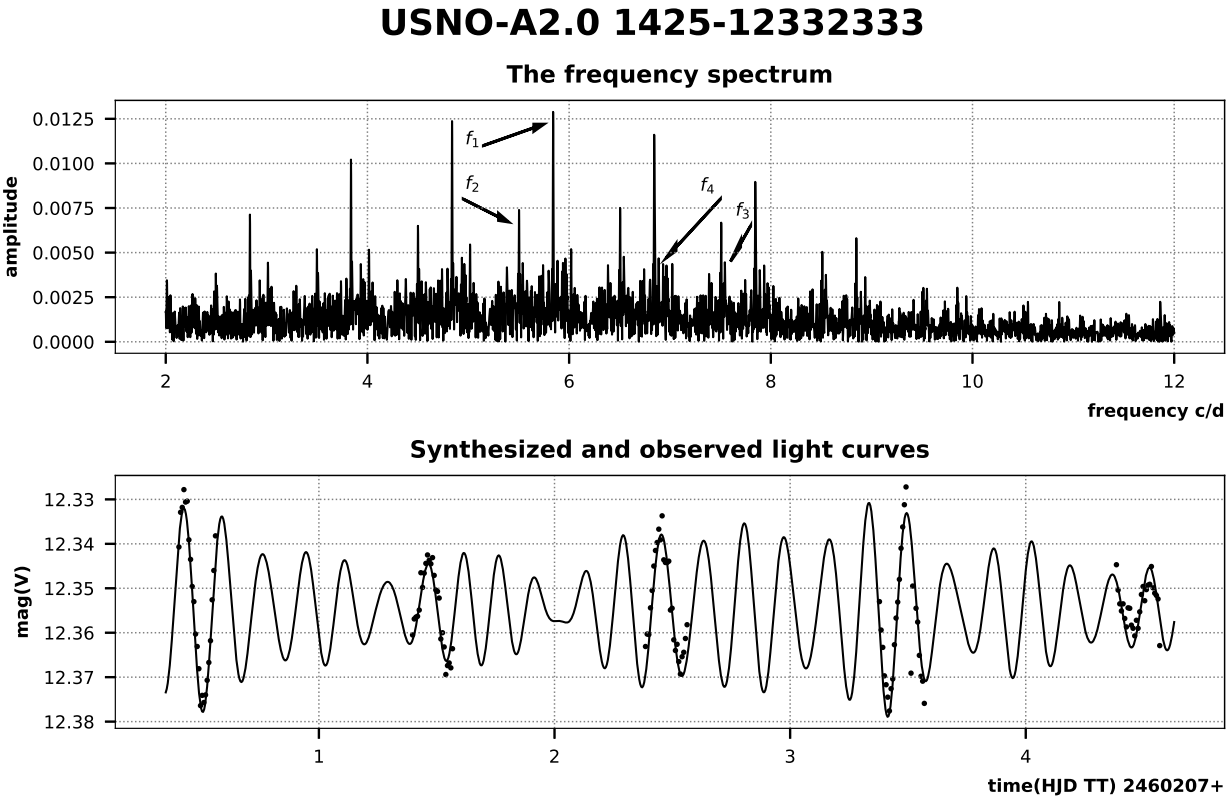

Figure 5.
The frequency spectrum and light curve of USNO-A2.0 1425-12332333. In the bottom panel, the solid curve is the synthesized light curve and dots are observed data points.

The finding chart based on a POSS2 red plate is presented in Fig. 6.

The phased V-band light curve of USNO-A2.0 1425-12332333 with the following light elements:

$$\text{Max HJD(TT)} = 2460207.4150 + 0^{\text{d}}.171196 \times E$$

is presented in Fig. 7.

3.3 USNO-A2.0 1425-12344159

The frequency spectrum of USNO-A2.0 1425-12344159 and its theoretical light curve (solid curve) with superposed data points corresponding to individual observations are given in Fig. 8. Light curve variations are easy to notice, they are reproduced with the model rather well.

The finding chart based on a POSS2 red plate is presented in Fig. 9.

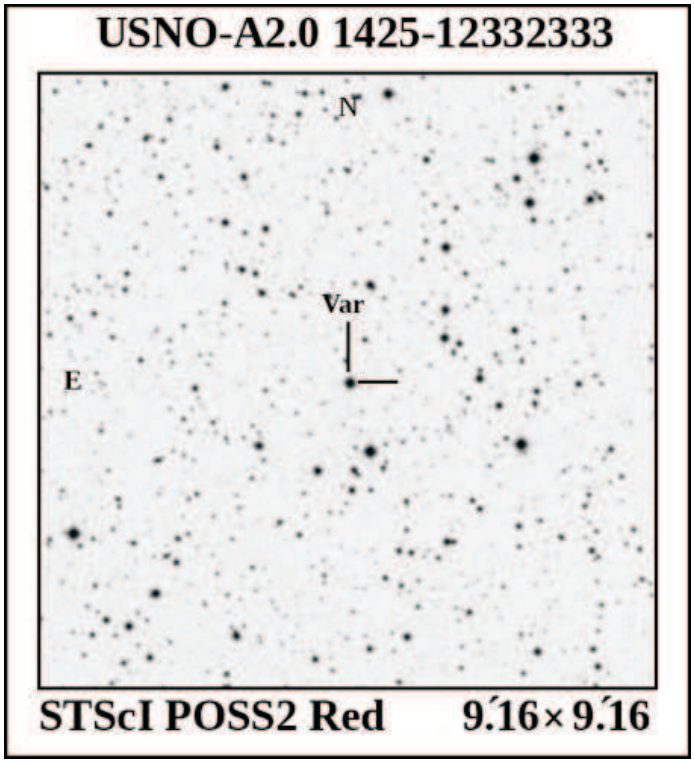

Figure 6.
A finding chart for USNO-A2.0 1425-12332333.

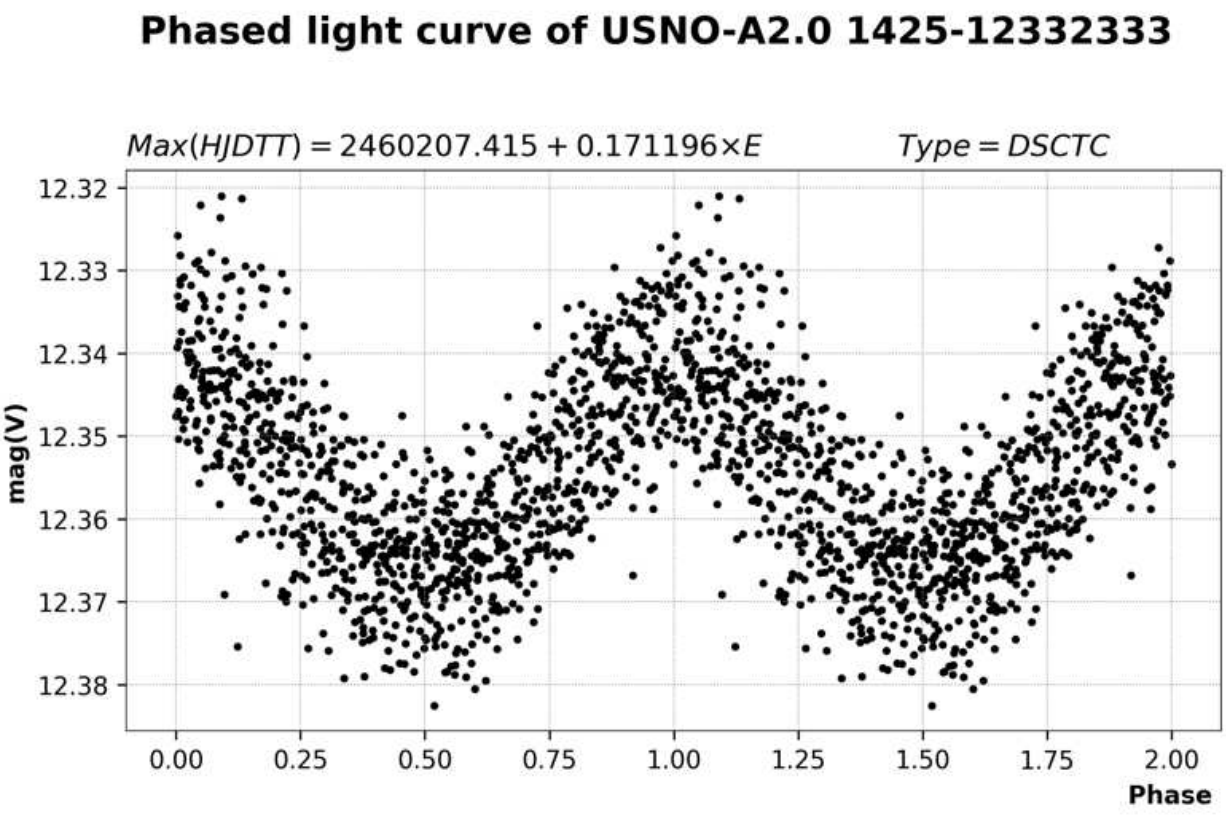

Figure 7.
Phased light curve of USNO-A2.0 1425-12332333.

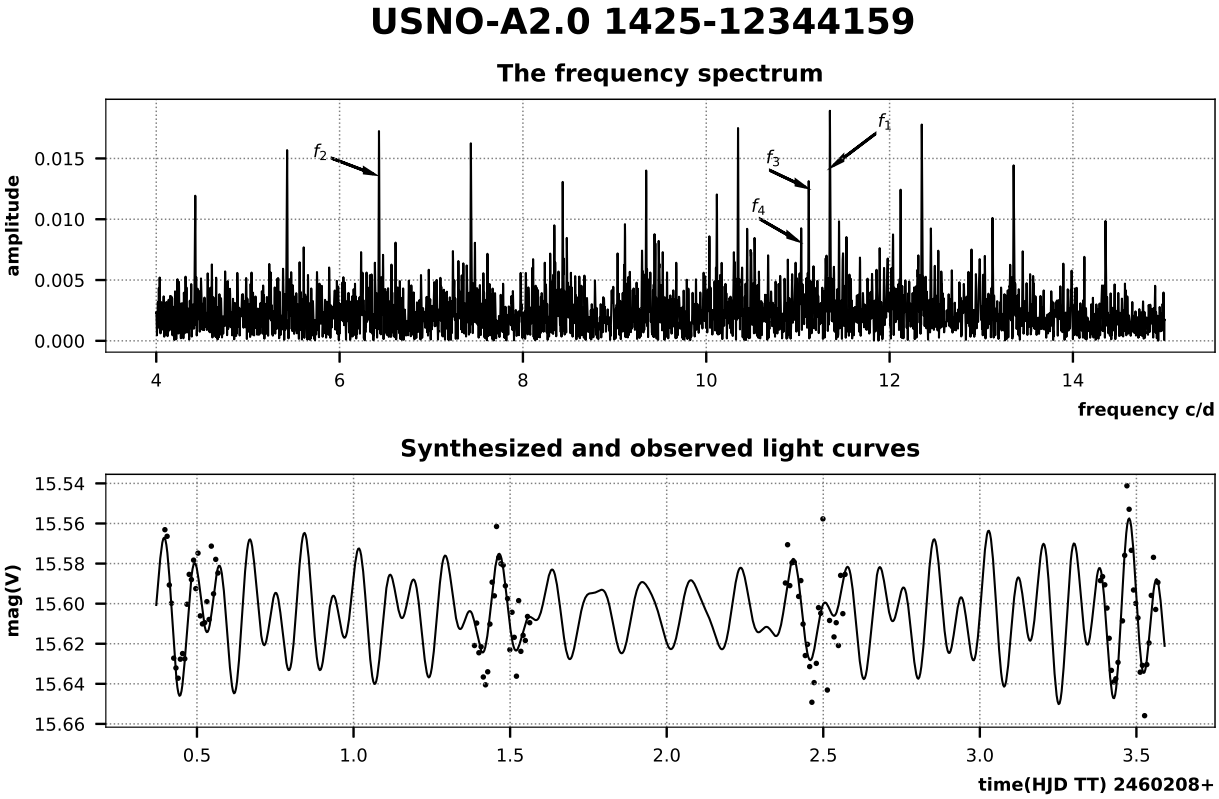

Figure 8.
The frequency spectrum and light curve of USNO-A2.0 1425-12344159. In the bottom panel, the solid curve is the synthesized light curve and dots are observed data points.

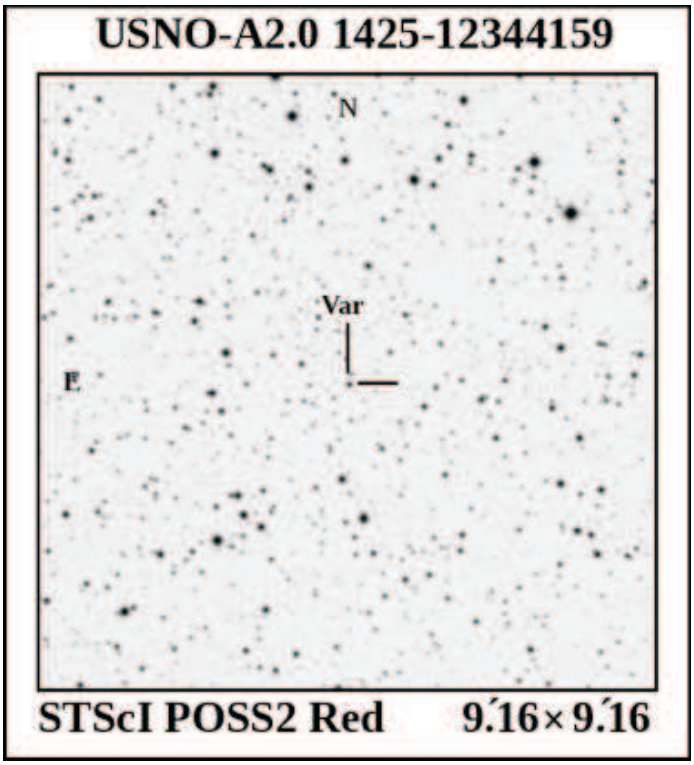

Figure 9.
A finding chart for USNO-A2.0 1425-12344159.

The phased V-band light curve of USNO-A2.0 1425-12344159 with the following light elements:

$$\text{Max HJD(TT)} = 2460208.3956 + 0^{\text{d}}.088112 \times E$$

is presented in Fig. 10.

3.4 USNO-A2.0 1425-12354548

Figure 11 presents the frequency spectrum of USNO-A2.0 1425-12354548 and its theoretical light curve (solid curve) with superposed data points corresponding to individual observations.

The finding chart based on a POSS2 red plate is presented in Fig. 12.

The phased V-band light curve of USNO-A2.0 1425-12354548 with the following light elements:

$$\text{Max HJD(TT)} = 2460230.3458 + 0^{\text{d}}.055766 \times E$$

is presented in Fig. 13.

3.5 USNO-A2.0 1425-12372223

Figure 14 presents the frequency spectrum of USNO-A2.0 1425-12372223 and its theoretical light curve (solid curve) with superposed data points corresponding to individual observations.

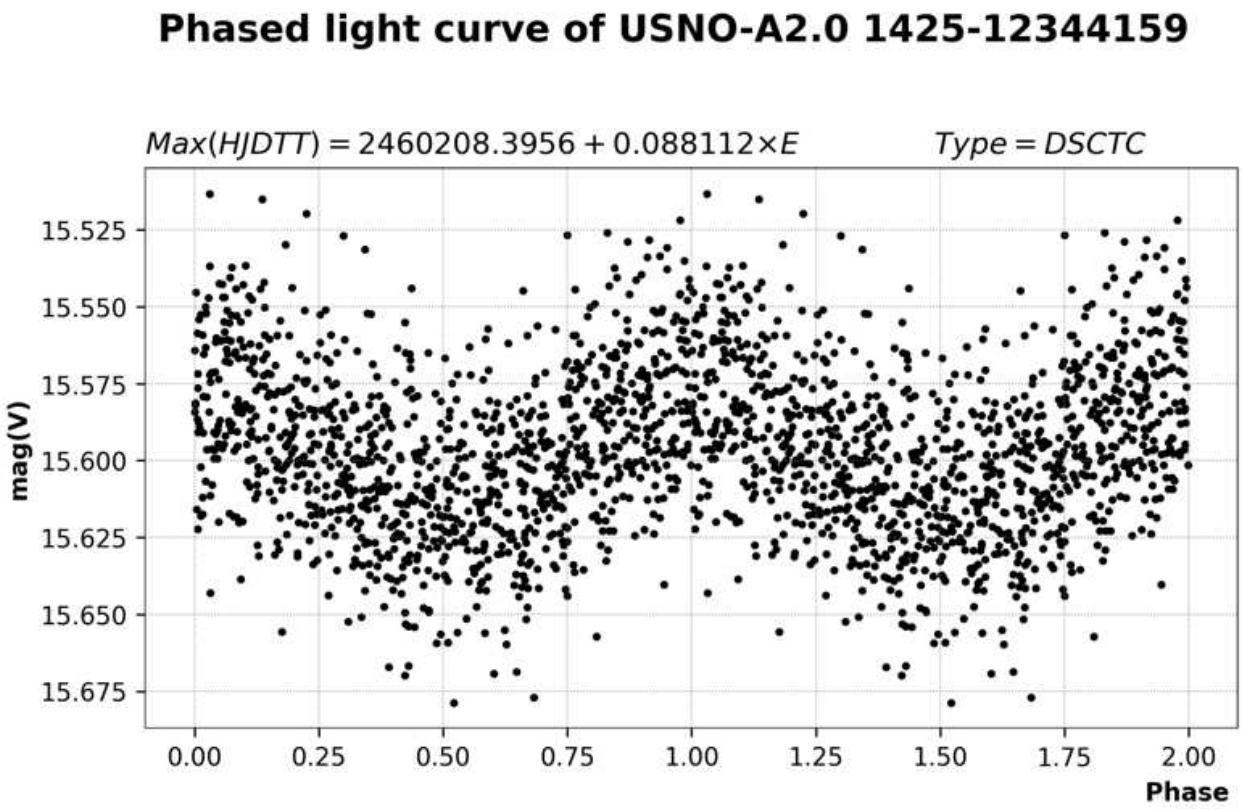

Figure 10.
Phased light curve of USNO-A2.0 1425-12344159.

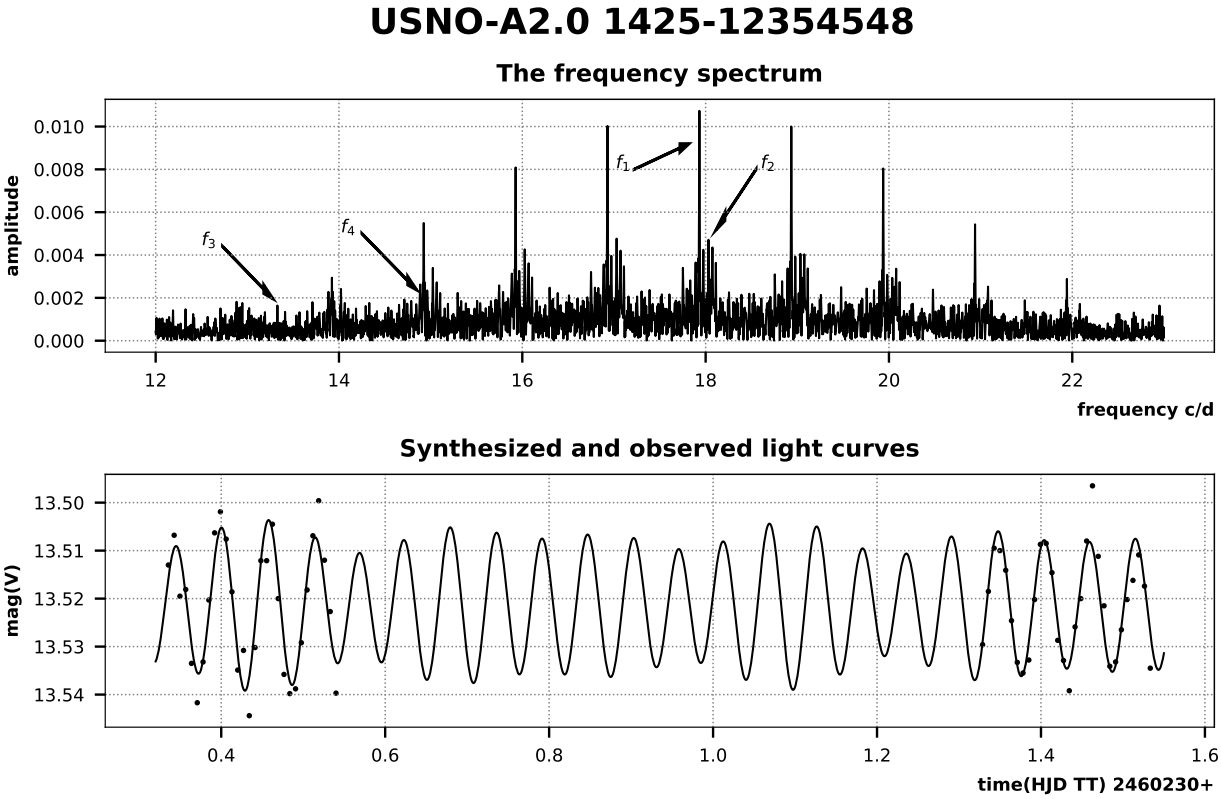

Figure 11.
The frequency spectrum and light curve of USNO-A2.0 1425-12354548. In the bottom panel, the solid curve is the synthesized light curve and dots are observed data points.

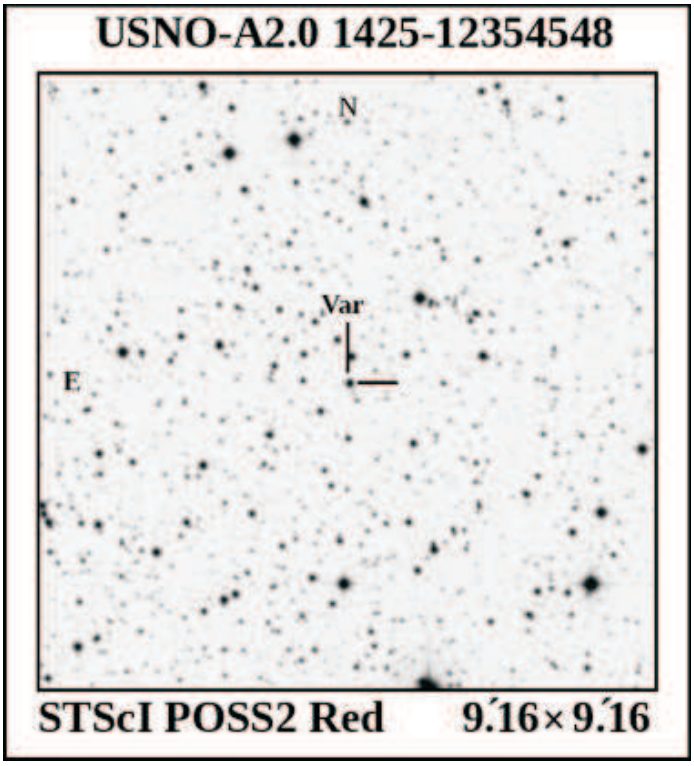

Figure 12.
A finding chart for USNO-A2.0 1425-12354548.

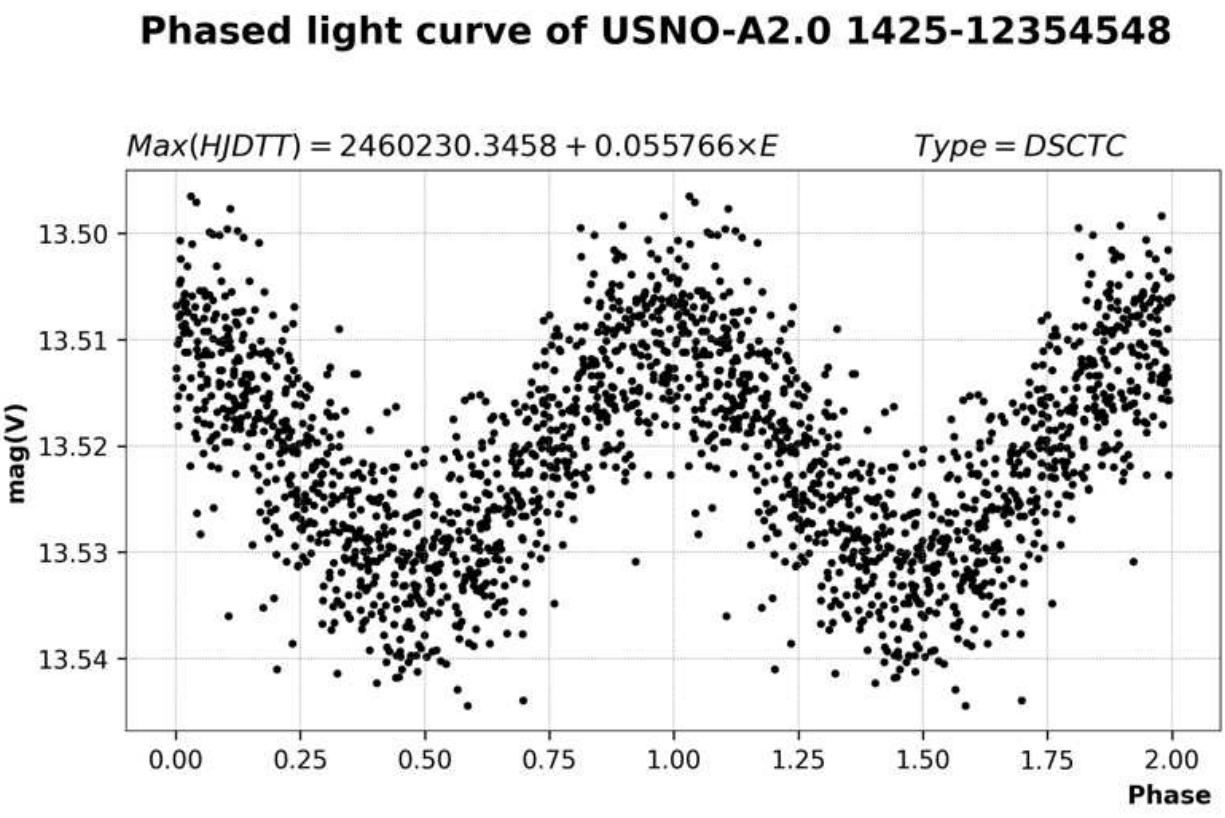

Figure 13.
Phased light curve of USNO-A2.0 1425-12354548.

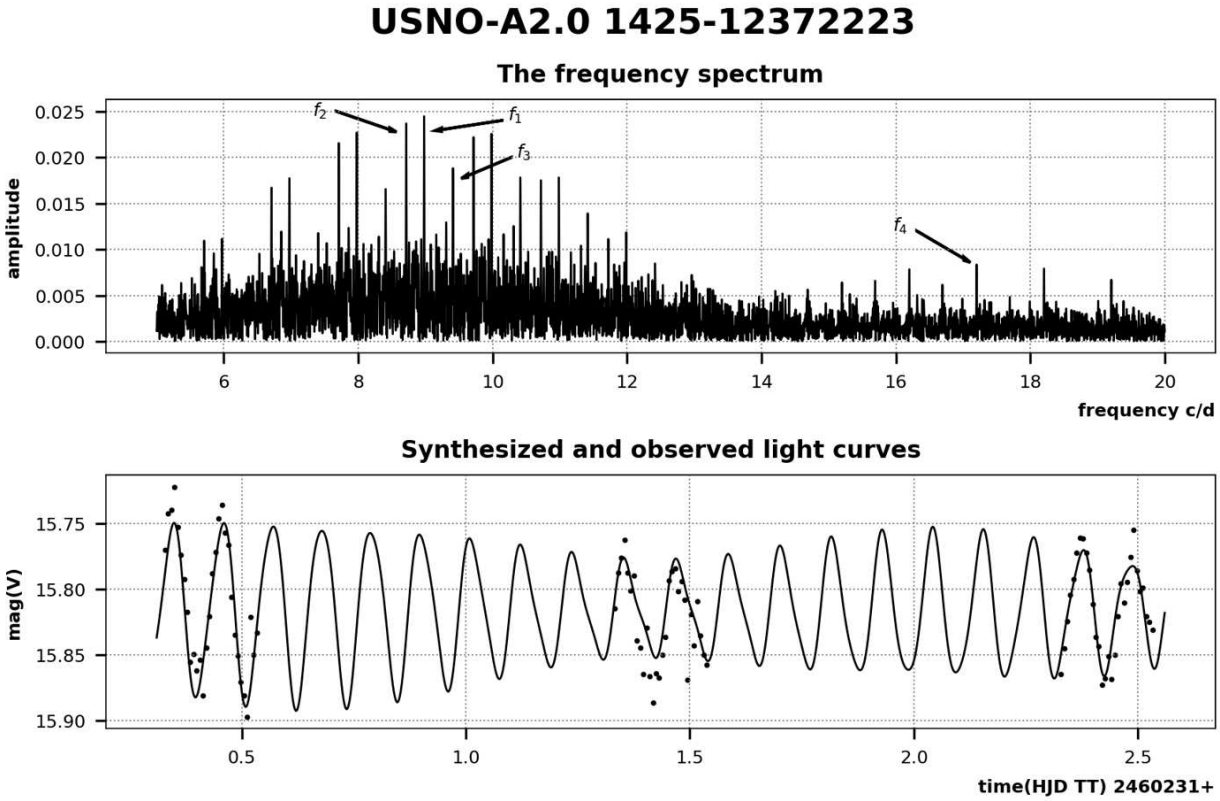

Figure 14.
Frequency spectrum and light curve of USNO-A2.0 1425-12372223. In the bottom panel, the solid curve is the synthesized light curve and dots are observed data points.

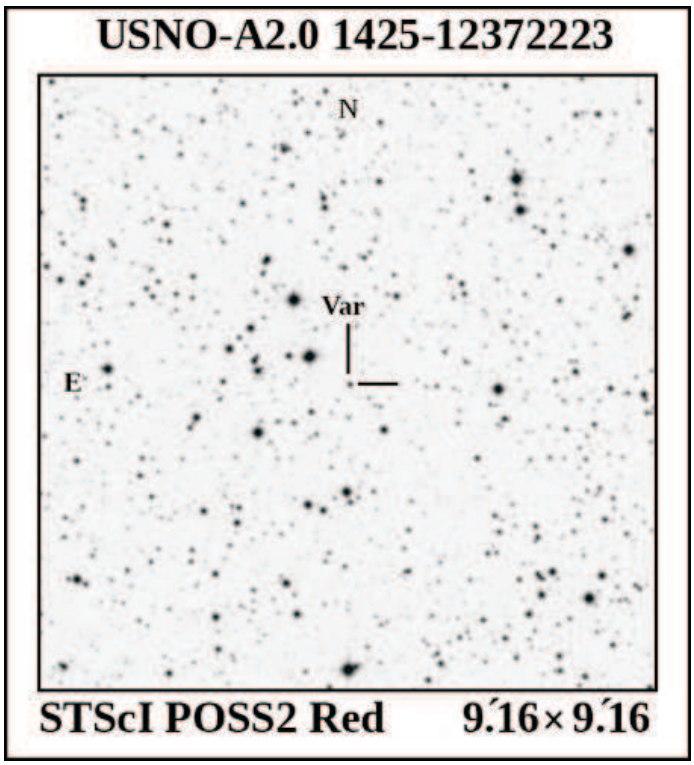

Figure 15.
A finding chart for USNO-A2.0 1425-12372223.

The finding chart based on a POSS2 red plate is presented in Fig. 15.

The V-band phased light curve of USNO-A2.0 1425-12372223 with the following light elements:

$$\text{Max HJD(TT)} = 2460208.5268 + 0\overset{\text{d}}{.}0.111365 \times E$$

is presented in Fig. 16.

3.6 USNO-A2.0 1425-12374410

Figure 17 presents the frequency spectrum of USNO-A2.0 1425-12374410 and its theoretical light curve (solid curve) with superposed data points corresponding to individual observations.

The finding chart based on a POSS2 red plate is presented in Fig. 18.

The phased V-band light curve of USNO-A2.0 1425-12374410 with the following light elements:

$$\text{Max HJD(TT)} = 2460231.3404 + 0\overset{\text{d}}{.}078946 \times E$$

is presented in Fig. 19.

3.7 USNO-A2.0 1425-12377701

Figure 20 presents the frequency spectrum of USNO-A2.0 1425-12377701 and its theoretical light curve (solid curve) with superposed data points corresponding to individual observations.

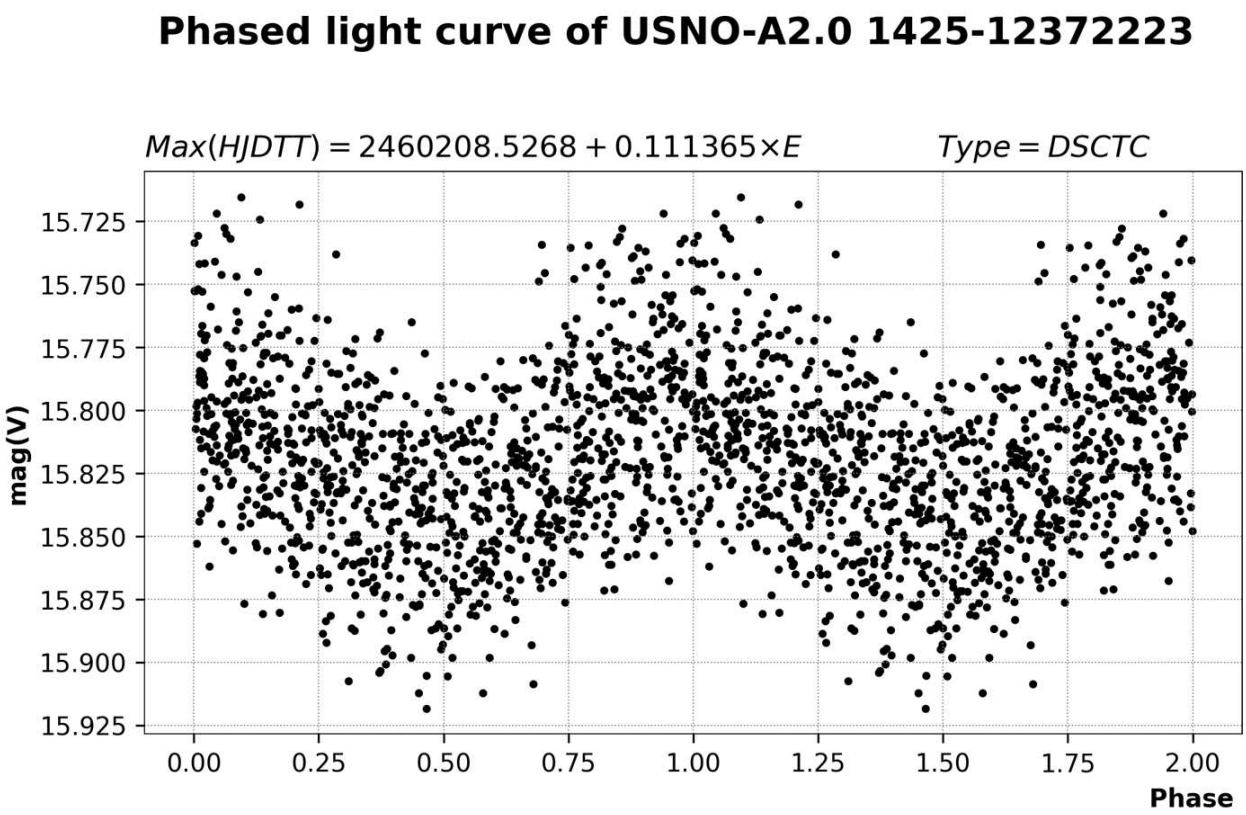

Figure 16.
Phased light curve of USNO-A2.0 1425-12372223.

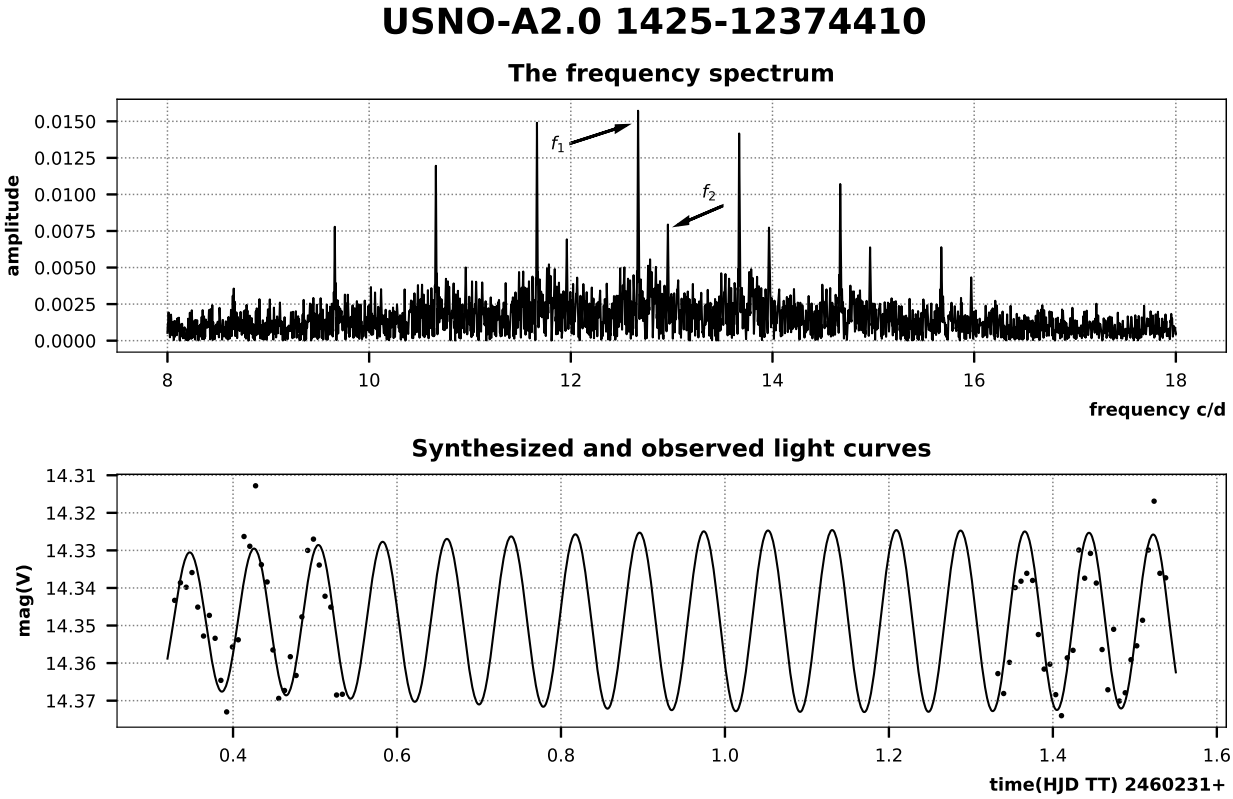

Figure 17.
The frequency spectrum and light curve of USNO-A2.0 1425-12374410. In the bottom panel, the solid curve is the synthesized light curve and dots are observed data points.

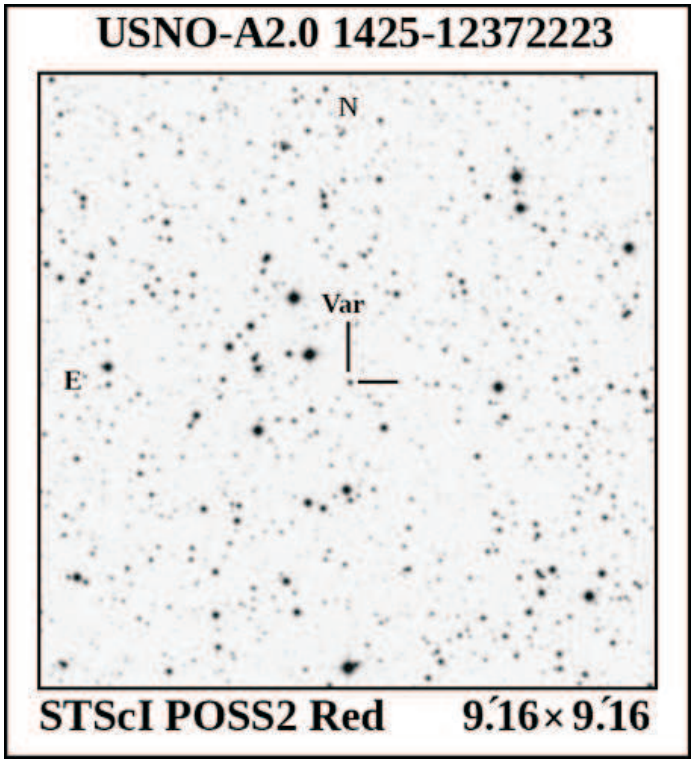

Figure 18.
A finding chart for USNO-A2.0 1425-12374410.

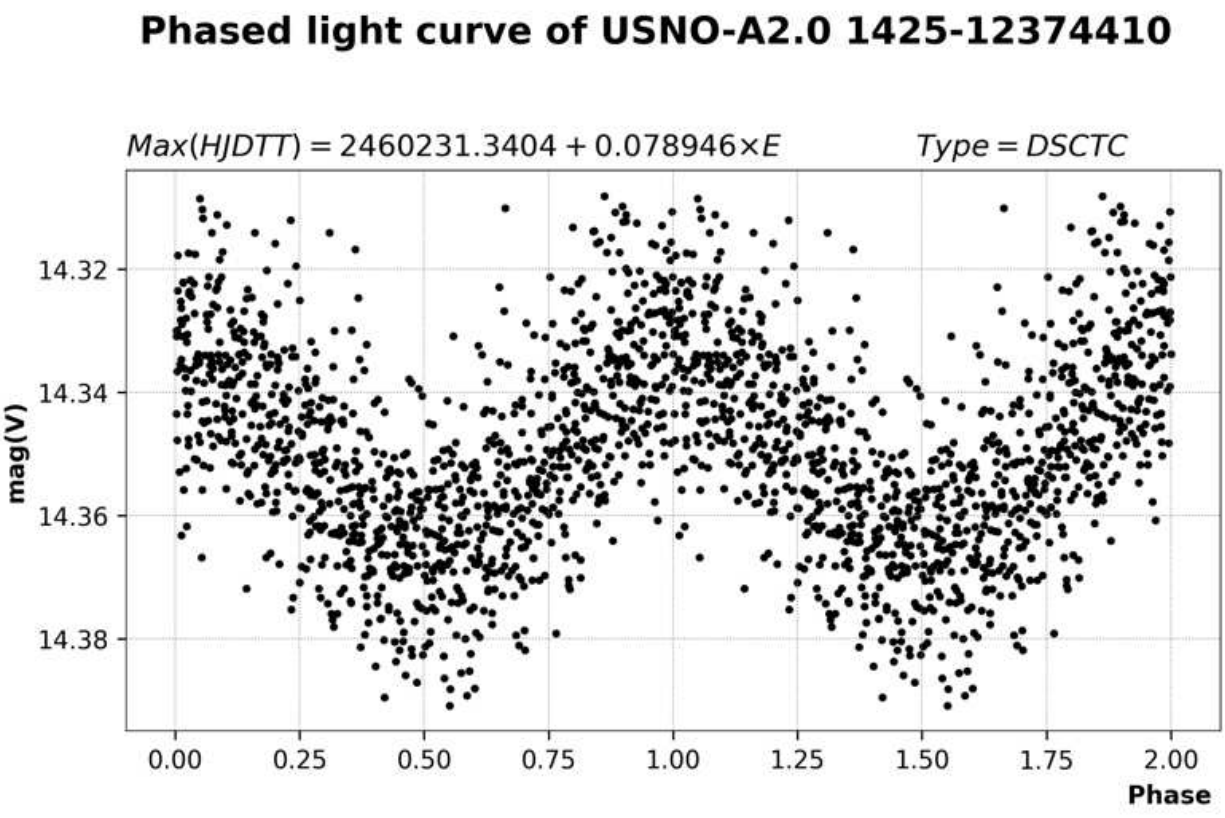

Figure 19.
Phased light curve of USNO-A2.0 1425-12374410.

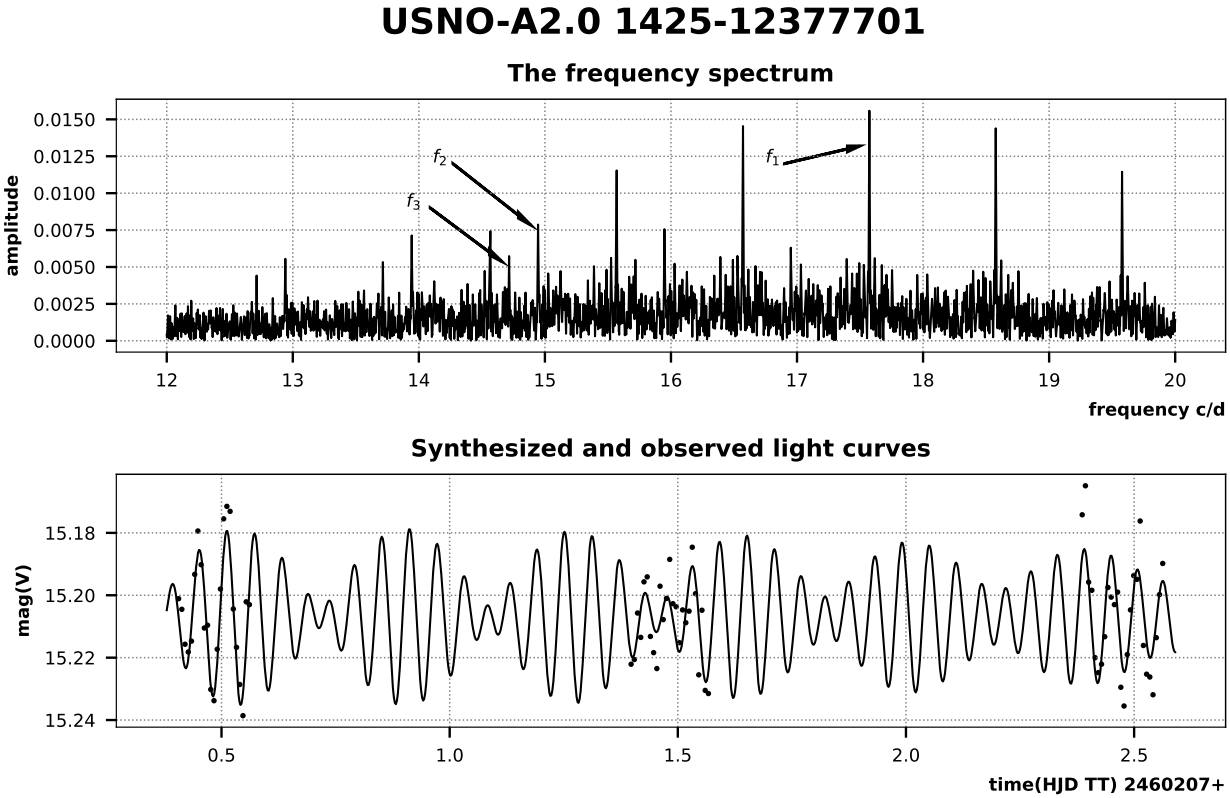

Figure 20.
The frequency spectrum and light curve of USNO-A2.0 1425-12377701. In the bottom panel, the solid curve is the synthesized light curve and dots are observed data points.

The finding chart based on a POSS2 red plate is presented in Fig. 21.

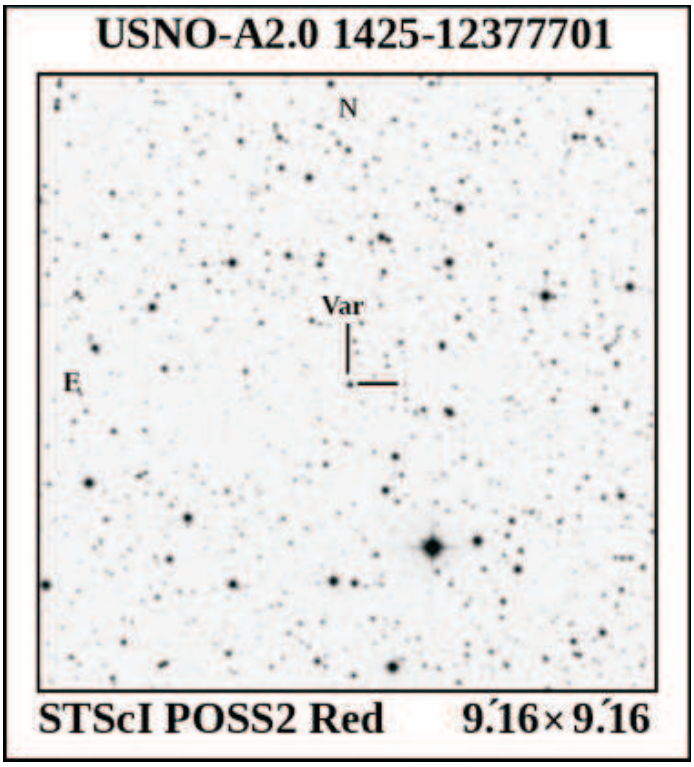

Figure 21.
A finding chart for USNO-A2.0 1425-12377701.

The phased V-band light curve of USNO-A2.0 1425-12377701 with the following light elements:

$$\text{Max HJD(TT)} = 2460207.4569 + 0^{\text{d}}.056902 \times E$$

is presented in Figure 22.

4 Conclusion

We have found seven new pulsating DSCTC stars with reliable signs of multiperiodic pulsations. All detected frequencies correspond to reliable oscillations.

The fact that the studied seven DSCTC stars are located in a small field (0.42 square degrees) is a good reason to continue the search for stars with similar pulsation properties at low galactic latitudes, in adjacent star fields.

In order to check for the presence of possible additional frequencies and to verify pulsation mode identification, new precision photometry in several standard photometric bands is needed. We appeal to observers having access to large telescopes to continue observations of these interesting variable stars.

Acknowledgements: I would like to thank Prof. N. N. Samus for helpful discussion and the anonymous referee for suggested improvements of the manuscript.

References:

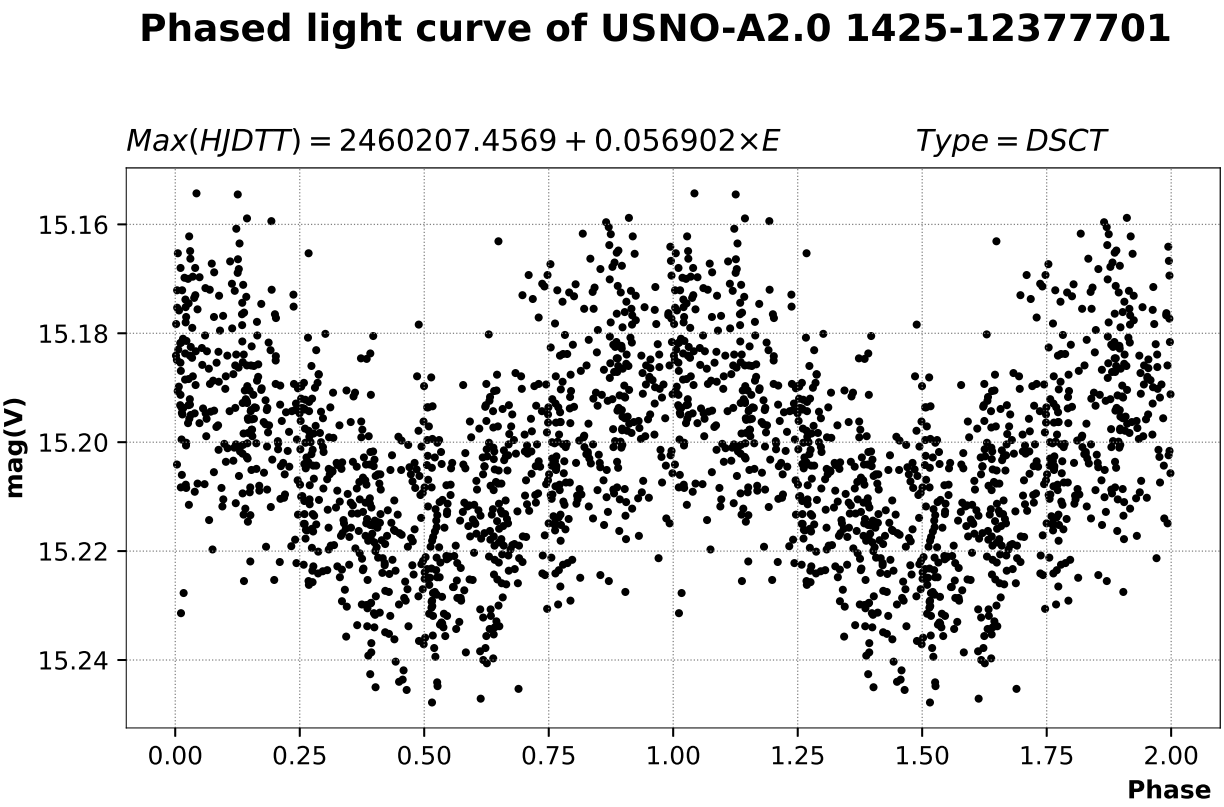

Figure 22.
Phased light curve of USNO-A2.0 1425-12377701.

Breger, M., 2000, *ASP Conference Series*, **210**, 3
Breger, M., Stich, J., Garrido, R., et al., 1993, *Astron. & Astrophys.*, **271**, 482
Cutri, R. M., Skrutskie, M. F., van Dyk, S., et al., 2003, *2MASS All Sky Catalog of Point Sources*, Centre de Données Astronomiques de Strasbourg, II/246
Eier, L., Audard, M., Holl, B., et al. 2023, *Astron. & Astrophys.*, **674**, article id. A13
Hunter, J. D., 2007, *Computing in Science & Engineering*, **9**, No. 3, 90
Harris, C. R., Millman, K. J., van der Walt, S. J., et al., 2020, *Nature*, **585**, 357
Lenz, P. & Breger, M. 2005, *Communications in Asteroseismology*, **146**, 53
Monet, D., Bird, A., Canzian, B., et al., 1998, *USNO-A V2.0, A Catalog of Astrometric Standards*, Centre de Données Astronomiques de Strasbourg, I/252
Samus, N. N., Kazarovets, E. V., Durlevich, O. V., Kireeva, N. N., Pastukhova, E. N., 2017, *Astron. Reports*, **61**, 80
Shatsky, N., Belinski, A., Dodin, A., et al., 2020, in *Ground-Based Astronomy in Russia. 21st Century*, ed. I. I. Romanyuk, I. A. Yakunin, A. F. Valeev, & D. O. Kudryavtsev, p. 127
Sokolovsky, K. V. & Lebedev, A. A., 2018, *Astron. and Computing*, **22**, 28
Watson, C. L., Henden, A. A., & Price, A., 2007, *Journal of the AAVSO*, **35**, 414